# LITHOSPHERIC MANTLE EVOLUTION IN THE AFRO-ARABIAN DOMAIN: INSIGHTS FROM BIR ALI MANTLE XENOLITHS (YEMEN)

PAOLO SGUALDO
Dipartimento di Fisica e Scienze della Terra, Università di Ferrara, Via Saragat 1, 44100 Ferrara

## INTRODUCTION

Mantle xenoliths exhumed from the Neogene-Quaternary alkaline volcanism in the Afro-Arabian domain provide a powerful tool to unravel the complex mantle dynamics in a region that was interested by plume-related Oligocene Continental Flood Basalt (CFB) magmatism (Hofmann *et al.*, 1997; Pik *et al.*, 1998; Beccaluva *et al.*, 2009) and rifting processes (Natali *et al.*, 2011, 2013a), from continental break-up to oceanization (Fig. 1).

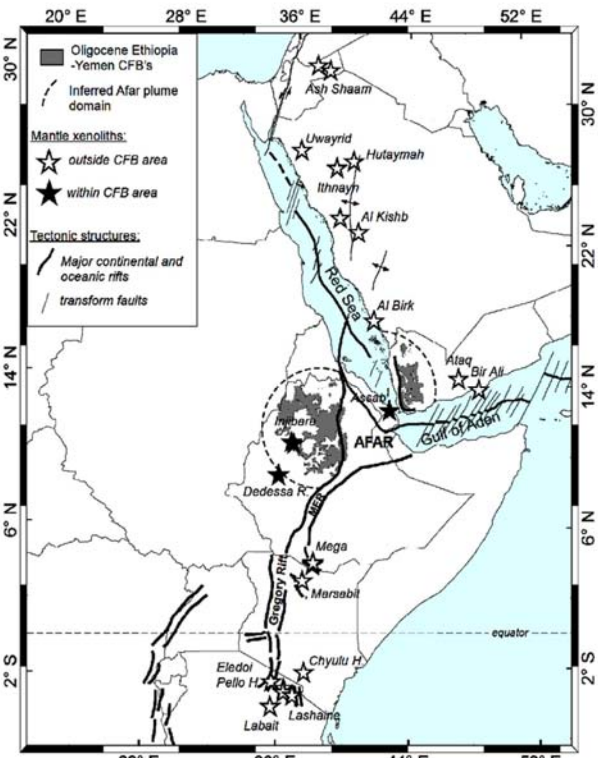


Fig. 1 - Sketch map of the Afro-Arabian domain with indication of Oligocene Continental Flood Basalts and the main mantle xenolith occurrences related to Neogene-Quaternary (Beccaluva *et al.*, 2009). The main tectonic lineaments are after Bosworth *et al.* (2005) and Rogers (2006).

The influence of the plume has been gradually vanishing over time, as suggested by seismic images of the Afar region, where transition from continental rifting to incipient oceanization has been studied in detail (Bastow *et al.*, 2011).

In the Afro-Arabian region, mantle xenoliths included in Neogene-Quaternary alkaline volcanics are found in two main occurrences: *i*) within the Northern Ethiopian-Yemen plateau area (Beccaluva *et al.*, 2011) and *ii*) outside this area, neighbouring the rift structures which radiate from the Afar triple junction along the Red sea-Gulf of Aden Arabian margins (Henjes-Kunst *et al.*, 1990; Blusztajn *et al.*, 1995; Chazot *et al.*, 1996; Baker *et al.*, 1998) and along the Main Ethiopian and Kenya-Tanzania rifts southward (Kaeser *et al.*, 2006; Aulbach *et al.*, 2011; Beccaluva *et al.*, 2011).

While mantle xenoliths related to the CFB area show evidence of pervasive refertilization by Afar plume melts (Beccaluva *et al.*, 2011), other mantle xenoliths collected outside this area, along the Arabian margin and the East Africa Rifts, display more complex history of depletion and enrichment events (Baker *et al.*, 1998; Reisberg *et al.*, 2004; Aulbach *et al.*, 2011).

In this paper we present new bulk rock and mineral major and trace element data as well as Nd-Hf-Pb-He isotope systematics from an exhaustive sampling (more than 60 samples) from Bir Ali (Yemen), which is a xenolith occurrence located in the southern Arabian margin, ca. 500 km eastward of CFB from the Ethiopian-Yemeni plateau.

The aim is to define: *i*) the real composition, on a statistical basis, of the lithospheric mantle section underlying the southern Arabian margin; *ii*) its secular variations in terms of depletion and enrichment processes; *iii*) the geochemical and isotopical signature of the metasomatic events in relation to the Afar plume influence.

## METHODS

Mantle xenoliths studied in this work have been collected from pyroclastic material of the Bir Ali diatreme, belonging to the Pliocene-Quaternary Balhaf Bir Ali alkaline volcanic province (Mallick *et al.*, 1990), which is located in the central southern part of Yemen (Fig. 1). 62 ultramafic xenoliths (up to 20 cm in size) unaffected by host basalt infiltration were selected for a detailed investigation. Samples were sliced and the freshest portions (weighting between 15 and 30 g) were crushed and then powdered in an agate mill. Major and trace elements (Ni, Co, Cr, V, and Sr) were analysed, on powder pellets, by X-ray fluorescence (XRF), using a wavelength-dispersive automated ARL Advant'X spectrometer at the Department of Earth Sciences of the Ferrara's University. Accuracy and precision for major elements are estimated as better than 3% for Si, Ti, Fe, Ca, and K, and 7% for Mg, Al, Mn, Na; for trace elements (above 10 ppm) they are better than 10%. The REE, Sc, Y, Zr, Hf, Nb, Ta, Th, and U were analysed (after HF-$HNO_3$ dissolution of rock powders in teflon beakers) by inductively coupled mass spectrometry (ICP-MS) at the Department of Physics and Earth Sciences of the Ferrara's University, using an X Series Thermo-Scientific spectrometer. Accuracy and precision, based on the replicated analyses of samples and standards, are estimated as better than 10% for all elements well above the detection limit. Mineral compositions were obtained at the CNR-IGG Institute of Padova with a Cameca SX-50 electron microprobe (fitted with four wavelength dispersive spectrometers) at an accelerating voltage of 15 kV and specimen current of 15 nA, using natural silicates and oxides as standards. Trace element analyses on pyroxenes were carried out at the CNR-IGG of Pavia by LAM ICP-MS, using an Elan DRC-e mass spectrometer coupled with a Q-switched Nd:YAG laser source (Quantel Brilliant). The spot diameter was typically 50 µm, and the CaO content was used as internal standard. Precision and accuracy, better than 10% for concentrations at ppm level, were assessed by repeated analyses of NIST SRM 612 and BCR-2 standards.

For the Nd-Hf-Pb isotopic analysis hand-picked clinopyroxene separates (weight of 100-300 mg) and bulk rock powders (weight of 300-600 mg) have been preliminarily prepared in laboratories of the Department of Earth Sciences at the University of New Hampshire. Samples were leached in hot (~ 120 °C) 6 N HCl to remove any surface contamination, following techniques outlined in Blichert-Toft & Albarède (2009). The resulting residues were subsequently digested in a mixture of concentrated HF-$HNO_3$. Lutetium (Lu) and hafnium (Hf) were separated as described by Blichert-Toft *et al.* (1997) and the Light Rare Earth Element (LREE) fraction recovered from the Lu-Hf separation protocol was further processed to separate and concentrate neodymium (Nd).

Isotopic measurements were carried out by the Nu Plasma HR multi-collector inductively coupled plasma mass spectrometer (MC-ICP-MS) at the Ecole Normale Supérieure in Lyon. Hafnium and Nd isotope analyses of samples were run in alternation with JMC-475 Hf and "Rennes" in-house Nd (courtesy C. Chauvel) standards, respectively and were normalized for mass fractionation relative to, respectively, $^{179}Hf/^{177}Hf = 0.7325$ and $^{146}Nd/^{144}Nd = 0.7219$ using an exponential law.

The 100-ppb JMC 475 Hf standard, run throughout the analytical session (n = 16) to monitor instrument performance, yielded $^{176}Hf/^{177}Hf = 0.282155$ (with external $2\sigma = 0.000010$).

Lead was separated using techniques based on those described in Bryce & DePaolo (2004), and Pb isotopic measurements were carried out on the Nu Plasma HR multi-collector inductively coupled plasma mass spectrometer (MC-ICP-MS) at the Ecole Normale Supérieure in Lyon. For Pb, mass fractionation was corrected via thallium normalization as described in White *et al.* (2000), and ratios were additionally adjusted for drift using the standard bracketing technique outlined in Albarède *et al.* (2004) using NIST SRM values reported in Eisele *et al.* (2003). Four NIST SRM 981 run as "blind" samples amongst the seventeen bracketing standards analyzed yielded averages (with $2\sigma$ external precision) of $^{208}Pb/^{204}Pb = 36.7271$ (0.0019), $^{207}Pb/^{204}Pb = 15.4978$ (0.0009) and $^{206}Pb/^{204}Pb = 16.9408$ (0.0012).

Helium was extracted from hand picked olivine crystals by in vacuo crushing and analysed at the laboratories of the Oregon University (US) using the procedure described by Graham *et al.* (1998).

PETROGRAPHY AND GEOCHEMISTRY

The composition in terms of the Ol-Opx-Cpx normative classification (following Niu., 1997; Fig. 2) shows that mantle xenoliths may be classified as spinel (Sp)-peridotites (35 lherzolites, 10 dunites and 6 harzburgites) and Sp-pyroxenites *s.l.* (5 ol-websterites and 5 websterites). Sp-peridotites are mainly protogranular in texture, only locally porphyroclastic and rarely equigranular. Olivine is generally medium to coarse grained (up to 2 mm) and moderately kink-banded, varying in composition from Fo 87.3 to Fo 92.0 in lherzolites, and from Fo 89.1 to Fo 92.9 in dunites. Orthopyroxene varies in size from medium to small grained, commonly showing cpx exolution *lamellae*; it ranges in composition from En 88.9 to En 92.5. Clinopyroxene is generally small grained and often interstitial, displaying opx exolution *lamellae* in the relatively largest crystals; its composition varies in the range En 49.1-52.9 Fs 0.5-3.0 Wo 45.4-48.7. Dark brown spinel is scarce, with lobate shape showing the following compositional ranges: Mg# 76-81 Cr# 11-27 in lherzolites, and Mg# 71-79 Cr# 17-38 in dunites. Interactions with metasomatising agents are evidenced by secondary minerals overimposed on the primary parageneses, particularly widespread in harzburgites and dunites. Reaction textures include "spongy" borders in clinopyroxene, opacized rims around spinel often containing fine-grained aggregates of secondary olivine and clinopyroxene as well as patches containing brownish to yellowish glass, rare plagioclase (An 52-70) and rare disseminated pargasitic amphibole (Mg# 88.8-88.9).

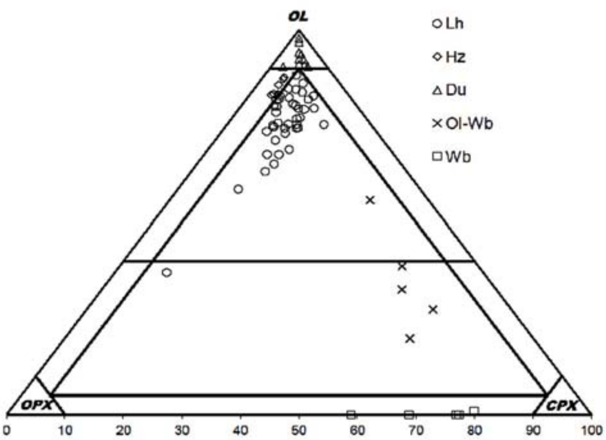


Fig. 2 - Composition of Bir Ali mantle xenoliths in terms of Ol-Opx-Cpx. Abbreviations: Lh = lherzolite; Hz = harzburgite; Du = dunite; Ol-Wb = olivine websterite; Wb = websterite; LOI = loss on ignition; Mg# = mol [MgO/(MgO+FeO)]; Ol = olivine; Opx = orthopyroxene; Cpx = clinopyroxene.

Sp-pyroxenites are represented either as individual xenoliths or as discrete domain texturally equilibrated inside peridotites. Like peridotites, pyroxenites exhibit prevalent protogranular texture, in place turning to porphyroclastic and equigranular, although with different composition of constituent minerals with respect to peridotites. Clinopyroxene is the dominant mineral phase, varying in composition between En 47.3 Fs 4.7 Wo 42.9 and En 51.5 Fs 7.0 Wo 47.6. Orthopyroxene composition is in the range En 83.8-85.9 Olivine is medium grained, weakly deformed and its composition varies in the range of Fo 82.2-83.9. Spinel is brown to dark green in color with Mg# 49-61 and Cr# 18-33. These compositions conform to those reported for analogous Bir Ali xenoliths by Ali & Arai (2007).

Thermo-barometric estimates for peridotites, based on the Brey & Kohler (1990) and Kohler & Brey, (1990) algorithms, indicate that Bir Ali mantle xenoliths equilibrated in a range of T (temperature) 900-1100 °C and P (Pressure) 9-20 Kbar, in agreement with those reported by Ali & Arai (2007) for Bir Ali, Stern & Johnson (2010) for the Arabian Peninsula, and by Conticelli *et al.* (1999) for Southern Ethiopia.

Peridotite xenoliths plot along the melting depletion trends with a continous $SiO_2$-CaO-$Al_2O$ and $TiO_2$ decrease from fertile lherzolites approaching the Primitive Mantle (PM) to extremely depleted dunites (Fig. 3). The restitic nature of these dunites after severe partial melting events is favored with respect to a replacive origin, such as that proposed for "dunite channels" in abyssal and ophiolite mantle peridotites (Suhr, 1999; Bernstein *et al.*, 2006; Piccardo *et al.*, 2007; Abily & Ceuleneer, 2013); this is supported by the lack of any chemical, modal and mineralogical compositional gap within the peridotite depletion trend.

Pyroxenites are remarkably displaced from PM indicating that significant chemical components such as $Al_2O_3$, CaO, $TiO_2$, and $K_2O$ variably enriched the pristine peridotite mantle section, possibly due to infiltration and interaction with basaltic melts (Fig. 3). The resulting compositions are perfectly comparable with those of pyroxenite mantle xenoliths from other occurrences of the Arabian peninsula (Stern & Johnson, 2010, and references therein), and conform to most pyroxenites occurring in ultramafic massifs, which are generally considered products of cumulus crystallization of basic melts intruding and interacting with the mantle peridotite (Downes, 2007). By contrast, Bir Ali pyroxenite xenoliths show remarkable differences with respect to those from the Northern Ethiopian plateau area (Injibara and Dedessa), which are comparatively enriched in orthopyroxene (Beccaluva *et al.*, 2011).

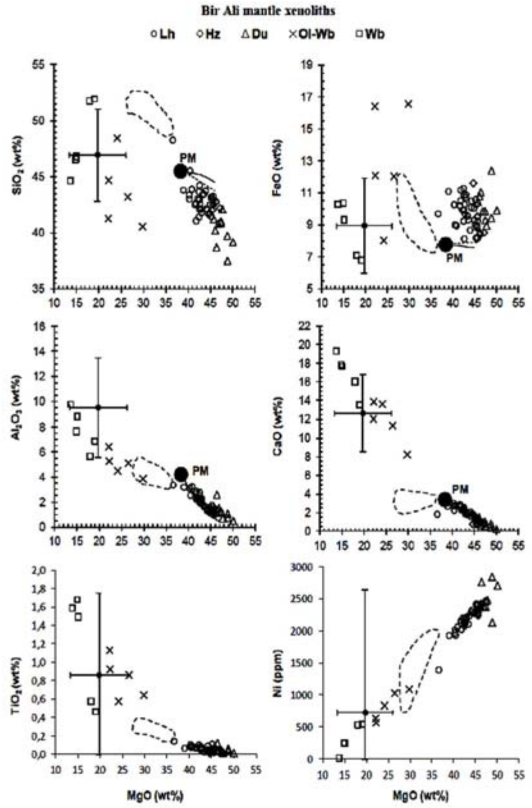


Fig. 3 - Variations diagrams of $SiO_2$, $TiO_2$, $Al_2O_3$, FeO, CaO and Ni *versus* MgO (wt.%) of mantle xenoliths from Bir Ali. Batch and fractional melting trends (dashed and continuous lines respectively) are reported after Niu (1997). Also reported for comparison average (± standard deviation) pyroxenite composition of mantle xenoliths from the Arabian Peninsula and the pyroxenite field (dashed field) from Dedessa and Injibara. Abbreviations as in Fig. 2.

Middle (M) and Heavy (H)-REE distribution of Bulk rock Chondrite (Ch)-normalized Rare Earth Elements (REE) of Bir Ali xenoliths is positively correlated with the modal clinopyroxene content, as usually observed in mantle rocks (Coltorti *et al.*, 1999; Beccaluva *et al.*, 2001, 2007, 2008, 2011). Accordingly, the M- and H-REE contents range from 0.4 to 1.9 times chondrite in lherzolites, from 0.3 to 0.5 in harzburgites and from 0.2 to 0.6 in most dunites.

A notable exception is represented by three dunites (characterized by abundant reaction textures and presence of glass and amphibole) which show M- and H-REE contents ranging from 0.7 to 1.4 times chondrite.

The enrichment in the most incompatible elements (*e.g.* Light (L) REE) is indicated by the $La_N/Yb_N$ ratio ranging from 0.3 to 2.0 in lherzolites, 0.4-2.6 in harzburgites and 0.7-4.1 in dunites, with the highest ratios corresponding to samples showing the most widespread reaction textures. Therefore, the $La_N/Yb_N$ ratio in peridotites may indicate that the interaction with metasomatic agents were slight or negligible in most lherzolites but much more effective in olivine-rich lithologies such as harzburgites and particularly dunites, as expected by experimental results on peridotite permeability (Toramaru & Fujii, 1986).

The reaction domains including newly formed mineral phases and glass indicate that interactions of peridotite matrix with metasomatic agents were relatively recent and did not attained textural re-equilibration.

Pyroxenites show HREE abundances ranging between 3.5 and 12.2 times chondrite, where the absolute REE concentrations increase from Ol-websterite to websterite. They display slightly positively fractionated REE patterns with $La_N/Yb_N$ increasing from 1.9 to 3.0, in broad relation with the abundance of modal clinopyroxene.

Ch-normalized REE distribution of clinopyroxene from Bir Ali mantle peridotites is reported in Fig. 4. Relatively homogeneous compositions are recorded within each sample, with patterns generally higher and subparallel to that of the relative bulk rock. M- to H-REE flat patterns are recorded in all clinopyroxenes ranging from 5.3 to 14.9 times chondrite. LREE distribution is highly variable with $La_N/Yb_N$ down to 0.2 for lherzolite unaffected by metasomatism, increasing up to 3.4 for those affected by metasomatic enrichment. As expected, clinopyroxenes in dunites record the most effective LREE metasomatic enrichment with $La_N/Yb_N$ up to 3.9.

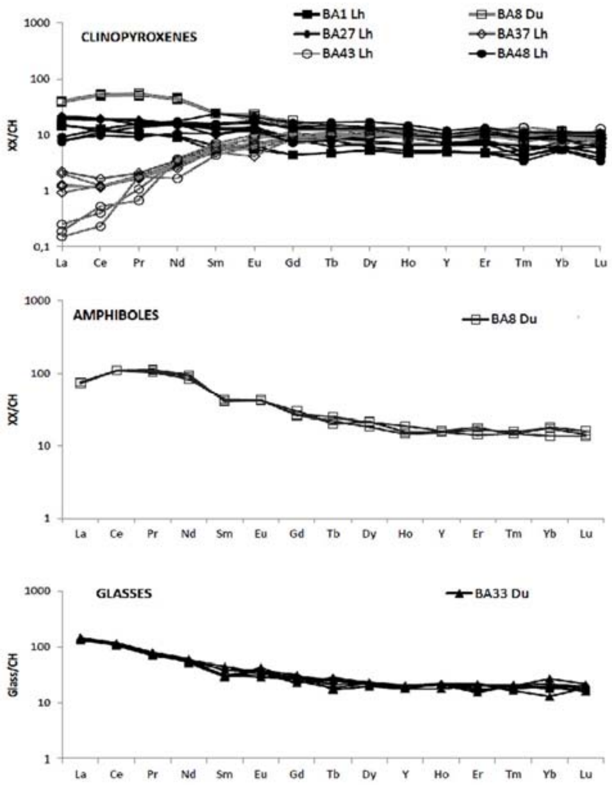


Fig. 4 - Chondrite-normalized REE distribution of clinopyroxene, amphibole and glass from Bir Ali mantle xenoliths. Normalizing factors are after Sun & McDonough (1989).

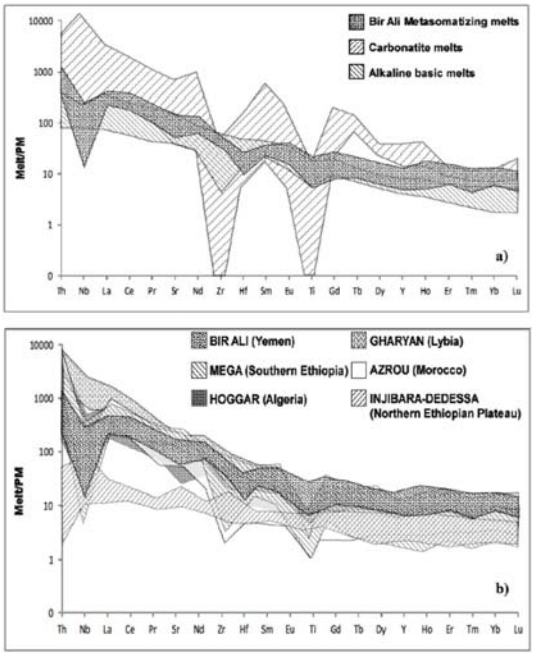


Fig. 5 - a) Primordial Mantle (PM) - normalized incompatible element patterns of the calculated metasomatic agents that affected mantle xenoliths from Bir Ali, compared with compositional envelopes of alkaline basic melts and carbonatites; b) PM - normalized incompatible element patterns of the calculated metasomatic agents of mantle xenoliths from Bir Ali compared with other Afro-Arabian mantle occurrences.

The amphibole REE patterns (in dunite BA8) is characterized by the M-HREE distribution ranges from 23.4 to 24.7 times chondrite and $La_N/Yb_N$ in the range 4.1-5.5. The related patterns mimic those of clinopyroxene from the same sample, suggesting that the two phases were reaction products of the same metasomatic agent. The REE distribution of glass (in dunite BA33) is characterized by HREE in the range of 18.6-21.9 times chondrite and positive fractionation, with $La_N/Yb_N$ averaging around 7.0. The above data coherently suggest that these new phases and the related geochemical enrichments were induced by alkali-silicatic metasomatic agents whose effects are evidenced by modal and textural disequilibrium. To constrain the nature of these metasomatising agents, incompatible element modelling has been performed based on the compositions of the most enriched clinopyroxene and pargasitic amphibole using partition coefficients (Kd) mineral/alkaline basic melt from Zack & Brumm (1998) and Dalpe & Baker (1994), respectively. The calculated metasomatising agents (Fig. 5) are in good agreement with the incompatible element distribution of basic alkaline lavas from Cenozoic volcanic districts of the African plate, whereas they do not fit with carbonatitic melts. Comparison at regional scale shows that metasomatic agents inferred for Bir Ali conform to those calculated for other mantle xenoliths occurrences of the Afro-Arabian domain, invariably characterized by alkali-silicate nature (Baker *et al.*, 1998; Beccaluva *et al.*, 2007, 2008, 2011; Natali *et al.*, 2013b). By contrast, mantle xenolith occurrences within the Northern Ethiopian Plateau area exhibit the interaction with subalkaline metasomatic agents, similar to CFB related to the Afar Plume activity (Beccaluva *et al.*, 2011).

## HF-ND-PB-HE ISOTOPES FROM BIR ALI XENOLITHS

Hf-Nd-Pb isotopic analyses were carried out on highly selected (hand-picked) clinopyroxene separates, and subordinately bulk rock powders, whereas He isotopic ratio was measured on olivine crystals. Results (Fig. 6) are discussed on the basis of the notional depleted (DM), high U/Pb (HIMU) and enriched (EM1, EM2) mantle components which refer to the different types of Ocean Island Basalts (OIB) and Mid Ocean Ridge Basalts (MORB) (Zindler & Hart, 1986; Carlson, 1995; Hofmann, 1997; Stracke *et al.*, 2005). The general distribution of Bir Ali peridotite xenoliths in terms of $^{143}$Nd/$^{144}$Nd-$^{176}$Hf/$^{177}$Hf span from the conventional Depleted Mantle (DM) signature or even more depleted compositions ( $\varepsilon_{Nd}$ up to 30.3 and $\varepsilon_{Hf}$ up to 64.4) to Enriched Mantle (EM) values ($\varepsilon_{Nd}$ down to -4.0 and $\varepsilon_{Hf}$ down to 4.0). The lherzolites are characterized by the most depleted supra-chondritic compositions, whereas harzburgites and dunites show enriched compositions coherent with the observed incompatible element distribution. This isotopic distribution confirms that lherzolites and harzburgites/dunites represent the least and most metasomatized peridotite mantle domains, respectively.

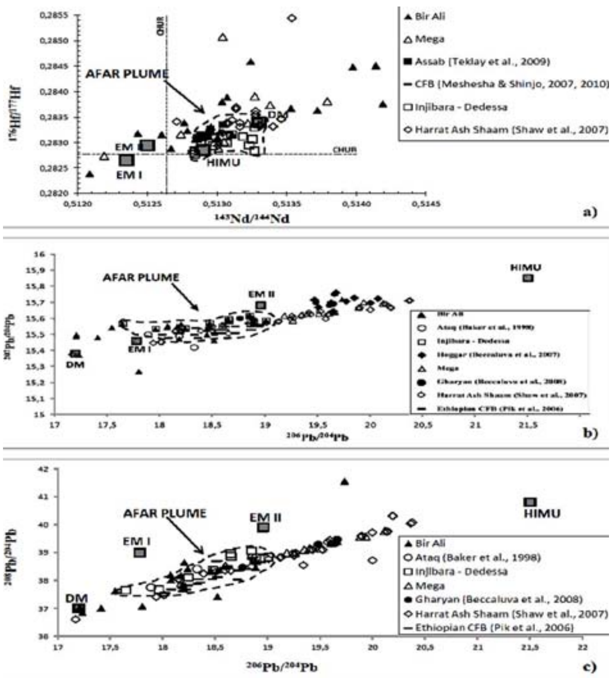


Fig. 6 - Hf-Nd (a) and Pb (b, c) isotopic compositions of bulk rock and clinopyroxene separates from Bir Ali mantle xenoliths, compared with those from other Afro-Arabian mantle occurrences.

The Model ages have been calculated on the basis of $^{176}$Hf/$^{177}$Hf and $^{143}$Nd/$^{144}$Nd respect to both CHUR and DM, for the most LREE depleted clinopyroxene of lherzolites BA37 and BA43. Hafnium model ages are in the range 2040-1800 and 1670-1115 Ma, respect to CHUR and DM. The Nd model ages are comparatively younger approaching 1300 (CHUR) and 1050 (DM) Ma. Therefore, from these estimates we may conclude that significant partial melting events took place during Proterozoic ages, and were followed by metasomatic interactions which variously perturbed the relative isotopic systems.

The Pb isotope systematic generally conforms to the above scenario with many lherzolites plotting close to DM, whereas harzburgites, dunites and websterites generally cluster near the EM components. In particular, the same lherzolites considered for the model ages are those showing unradiogenic Pb isotopic composition, thus confirming that they escaped significant metasomatic effects. More radiogenic Pb compositions are displaced toward the EM2 isotopic end-member. For comparison we report the isotopic compositions of mantle xenoliths from other localities of the Arabian plate (Ataq; Baker *et al*., 1998; Shaw *et al*., 2007), East Africa (Mega, Southern Ethiopia; author's data; Assab, Eritrea; Teklay *et al*., 2010; Injibara and Dedessa, Northern Ethiopia; author's data) and from the Saharan Belt (Hoggar, Algeria: Beccaluva *et al*., 2007; Gharyan, Lybia: Beccaluva *et al*., 2008). The resulting distribution show that the depletion and enrichment prcesses that affected the Afro-Arabian lithospheric domain produced an extreme variability of isotopic signatures, extending sometimes beyond the mantle arrays defined by the conventional mantle isotopic components (DM, EM and HIMU).

A relevant exception is represented by mantle xenoliths located within Northern Ethiopian-Yemeni plateau (Assab, Injibara and Dedessa), showing a relative isotopic homogeneity ($^{176}$Hf/$^{177}$Hf = 0.28277-0.28340, $^{143}$Nd/$^{144}$Nd = 0.51284-0.51329, $^{208}$Pb/$^{204}$Pb = 37.7-39.1, $^{207}$Pb/$^{204}$Pb = 15.5-15.6, $^{206}$Pb/$^{204}$Pb = 17.7-19.0), possibly inherited by pervasive interaction of these mantle sections with Afar plume-related CFB which display similar isotopic composition ($^{176}Hf/^{177}Hf$ = 0.28290-0.28319, $^{143}Nd/^{144}Nd$ = 0.51284-0.51307, Meshesha & Shinjo, 2007, 2010; $^{208}Pb/^{204}Pb$ = 37.6-39.1, $^{207}Pb/^{204}Pb$ = 15.4-15.7, $^{206}Pb/^{204}Pb$ = 18.0-19.3; author's data and Pik *et al*., 2006).

The helium isotope composition ($^{3}He/^{4}He$) of the olivines from Bir Ali varies from 7.5 to 7.8 Ra falling in the range recorded in other occurrences of the East African-Arabian domain (*e.g.*, Mega, Injibara, and Dedessa: 6.9-8.9, Beccaluva *et al*., 2011) and is systematically higher than that measured in peridotite xenoliths from Saharan belts (6.2-6.8; Azrou, Morocco: Natali *et al*., 2013b; Hoggar: Beccaluva *et al*., 2007; Gharyan: Beccaluva *et al*., 2008). A possible explanation is provided by the extreme mobility (and decoupling) of noble gases with respect to other incompatible elements, which may result in a much more extended lithospheric region influenced by the plume.

## CONCLUSIONS

The extensive sampling of mantle xenoliths from Bir Ali show that spinel-peridotites represent the preponderant part (85%) of the southern Arabian lithosphere, the remaining part (15%) being constituted by spinel-pyroxenites sometimes forming texturally equilibrated composite xenoliths. Peridotites exhibit a compositional variation from lherzolites (up to 14% clinopyroxene) to harzburgites and dunites (cpx down to 2-3%) which delineate a continuous depletion trend attributable multiple and intensive extraction of basic melts. The calculated model ages suggest that these partial melting events occurred at least since Paleo-Proterozoic (2 Ga according to Lu-Hf model age of the most depleted peridotites). Moreover, The Lu-Hf and Sm-Nd error-chrones calculated on the total xenoliths population suggest important magmatic events between 800 and 750 Ma. While the Paleo-Proterozoic ages may indicate the occurrence of extensive partial melting events in the pristine mantle, the Neo-Proterozoic ages may correspond to Pan-African magmatic events that modified the lithospheric mantle, as suggested by Stern & Johnson (2010). In our view, texturally equilibrated pyroxenites, which represent ubiquitous and significant components of mantle xenoliths throughout the Arabian Peninsula, could be related to these Neo-Proterozoic events that extensively rejuvenated the Arabian lithospheric mantle.

On the other hand, the observed disequilibrium textures and formation of new phases (glass, clinopyroxene and amphibole) in parallel with incompatible elements and isotopic enrichments could be derived by interactions with much younger and recent metasomatic agents that variously affected the studied lithospheric section. These metasomatic effects, particularly effective in harzburgite and dunite lithologies, indicate that the causative agents were OIB-type alkaline basic melts. Therefore, the Bir Ali mantle section, compared with others from the Afro-Arabian domain, confirms that the general extensional regime radiating from the Afar triple junction and generating the Red Sea-Gulf of Aden-Main Ethiopian Rift system, was accompanied by shallow mantle upwelling events and metasomatic processes dominated by alkaline agents (Henjes-Kunst *et al*., 1990; Kaeser *et al*., 2006; Bedini *et al*., 1997; Shaw *et al.*, 2007; Aulbach *et al*., 2011; Beccaluva *et al*., 2011). A notable exception is represented by mantle xenoliths included in Neogene-Quaternary alkaline volcanics located within the Northern Ethiopian-Yemeni CFB province; in these xenoliths, petrological and geochemical evidences indicate that the causative agents of mantle metasomatism were subalkaline melts closely resembling the tholeiitic magmas related to the Afar plume (Beccaluva *et al*., 2011 and references therein). We may conclude that the thermo-chemical effects of the Afar plume were essentially confined to the lithospheric sections located within the northern Ethiopian-Yemeni CFB plateau, and were negligible in the neighbouring regions. However, based on the available data on extremely mobile elements such as noble gases, we emphasize a regional scale anomaly throughout the East-African-Arabian domain showing a systematic higher Helium isotopic composition with respect to other African occurrences (residual plume influence?).

## REFERENCES

Abily, B. & Ceuleneer, G. (2013): The dunitic mantle-crust transition zone in the Oman ophiolites: residue of melt-rock interaction, cumulates from high-MgO melts, or both? *Geology*, **41**, 67-70.

Albarède, F., Telouk, P., Blichert-Toft, J., Boyet, M., Agranier, A., Nelson, B. (2004): Precise and accurate isotopic measurements using multiple-collector ICPMS. *Geochim. Cosmochim. Acta*, **68**, 2725-2744.

Ali, M & Arai, S. (2007): Clinopyroxene-rich lherzolite xenoliths from Bir Ali, Yemen - possible product of peridotite/melt reactions. *J. Miner. Petrol. Sci*., **102**, 137-142.

Aulbach, S., Rudnick, R.L., McDonough, W.F. (2011): Evolution of the lithospheric mantle beneath the East African Rift in Tanzania and its potential signatures in rift magmas. *GSA Sp. Pap.*, **478**, 105-125.

Baker, J.A., Chazot, G., Menzies, M., Thirlwall, M. (1998): Metasomatism of the shallow mantle beneath Yemen by the Afar plume - Implications for mantle plumes, flood volcanism, and intraplate volcanism. *Geology*, **26**, 431-434.

Bastow, I.D., Keir, D., Daly, E. (2011): The Ethiopia Afar Geoscientific Lithospheric Experiment (EAGLE): Probing the transition from continental rifting to incipient seafloor spreading. *GSA Sp. Pap.*, **478**, 51-76.

Beccaluva, L., Bianchini, G., Coltorti, M., Perkins, W.T., Siena, F., Vaccaro, C., Wilson, M. (2001): Multistage evolution of the European lithospheric mantle: new evidence from Sardinian peridotite xenoliths. *Contrib. Mineral. Petrol*., **142**, 284-297.

Beccaluva, L., Azzouni-Sekkal, A., Benhallou, A., Bianchini, G., Ellam, R.M., Marzola, M., Siena, F., Stuart, F.M. (2007): Intracratonic asthenosphere upwelling and lithosphere rejuvenation beneath the Hoggar swell (Algeria): evidence from HIMU metasomatised lherzolite mantle xenoliths. *Earth Planet. Sci. Lett.*, **260**, 482-494.

Beccaluva, L., Bianchini, G., Ellam, R., Marzola, M., Oun, K.M., Siena, F., Stuart, F.M. (2008): The role of HIMU metasomatic components in the African lithospheric mantle: petrological evidence from the Gharyan peridotites xenoliths, NW Libya. *In*: Mantle metasomatismo in intra-plate and suprasubduction setting. M. Coltorti and M. Grégoire, eds., *Geol. Soc. London, Spec. Publ.*, **293**, 253-277.

Beccaluva, L., Bianchini, G., Natali, C., Siena, F. (2009): Continental flood basalts and mantle plumes: a case study of the northern Ethiopian plateau. *J. Petrol.*, **50**, 1377-1403.

Beccaluva, L., Bianchini, G., Ellam, R.M., Natali, C., Santato, A., Siena, F., Stuart, F.M (2011): Peridotite xenoliths from Ethiopia: inferences about mantle processes from plume to rift settings. *GSA Sp. Pap.*, **478**, 77-104.

Bedini, R.M., Bodinier, J.-L., Dautria, J.-M., Morten, L. (1997): Evolution of LILE-enriched small melt fractions in the lithospheric mantle: a case study from the East African Rift. *Earth Planet. Sci. Lett.*, **53**, 67-83.

Bernstein, S.K., Hanghoj, K., Kelemen, P.B., Brooks, C.K. (2006): Ultra-depleted, shallow cratonic mantle beneath West Greenland: dunitic xenoliths from Ubekend Ejland. *Contrib. Mineral. Petrol*., **152**, 335-347.

Blichert-Toft, J. & Albarède, F. (2009): Mixing of isotopic heterogeneities in the Mauna Kea plume conduit. *Earth Planet. Sci. Lett.*, **282**, 190-200.

Blichert-Toft, J., Chauvel, C., Albarède, F. (1997): Separation of Hf and Lu for high-precision isotope analysis of rock samples by magnetic sector-multiple collector ICP-MS. *Contrib. Mineral. Petrol.*, **127**, 248-260.

Blusztajn, J., Hart, S.R., Shimizu, N., McGuire, A.V. (1995): Trace-element and isotopic characteristics of spinel peridotite xenoliths from Saudi Arabia. *Chem. Geol.*, **123**, 53-65.

Bosworth, W., Huchon, P., McClay, K. (2005): The Red Sea and Gulf of Aden Basins*. J. Afr. Earth Sci.*, **43,** 334-378.

Brey, G.P. & Kohler, T.P. (1990): Geothermobarometry in four phases lherzolites II. New thermobarometers and practical assessment of existing thermobarometers. *J. Petrol.*, **31**, 1353-1378.

Bryce, J.G. & DePaolo, D.J. (2004): Pb isotopic heterogeneity in basaltic phenocrysts. *Geochim. Cosmochim. Acta*, **68**, 4453-4468.

Carlson, R.W. (1995): Isotopic inferences on the chemical structure of the mantle. *J. Geodyn*., **20**, 365-386.

Chazot, G., Menzies, M., Harte, B. (1996): Silicate glasses in spinel lherzolites from Yemen: origin and chemical composition. *Chem. Geol.*, **134**, 159-179.

Coltorti, M., Bonadiman, C., Hinton, R.W., Siena, F., Upton, B.G.J. (1999): Carbonatite metasomatism of the Oceanic Upper Mantle: evidence from clinopyroxenes and glasses in ultramafici xenoliths of Grande Comore, Indian Ocean. *J. Petrol.*, **40**, 133-165.

Conticelli, S., Sintoni, M.F., Abebe, T., Mazzarini, F., Manetti, P. (1999): Petrology and geochemistry of ultramafic xenoliths and host lavas from the Ethiopian Volcanic Province: an insight into the upper mantle under eastern Africa. *Acta Vulcanol*., **11**, 143-159.

Dalpe, C. & Baker, D.R. (1994): Partition coefficients for rare-earth elements between calcic amphibole and Ti-rich basanitic glass at 1,5 Gpa, 1100 degrees C. *Mineral. Mag*., **58**, 207-208.

Downes, H. (2007): Origin and significance of spinel and garnet pyroxenites in the shallow lithospheric mantle: ultramafic massifs in orogenic belts in Western Europe and NW Africa. *Lithos*, **99**, 1-24.

Eisele, J., Abouchami, W., Galer, S.J.G., Hofmann, A.W. (2003): The 320 kyr Pb isotope evolution of Mauna Kea lavas recorded in the HSDP-2 drill core. *Geochem, Geophys. Geosyst.*, **4**, 8710.

Graham, D.W., Larsen, L.M., Hanan, B.B., Storey, M., Pedersen, A.K., Lupton, J.E. (1998): Helium isotope composition of the early Iceland mantle plume inferred from the Tertiary picrites of West Greenland. *Earth Planet. Sci. Lett.*, **160**, 241-255.

Henjes-Kunst, F., Altherr, F., Baumann, A. (1990): Evolution and composition of the lithospheric mantle underneath the western Arabian peninsula: constraints from Sr-Nd and type systematics of mantle xenoliths. *Contrib. Mineral. Petrol.*, **105**, 460-472.

Hofmann, A.W. (1997): Mantle geochemistry: the message from oceanic volcanism. *Nature*, **385**, 219-229.

Hofmann, C., Courtillot, V., Féraud, G., Rochette, P., Yirgu, G., Ketefo, E., Pik, R. (1997): Timing of the Ethiopian flood basalt event and implications for plume birth and global change. *Nature*, **389**, 838-841.

Kaeser, B., Kalt, A., Pettke, T. (2006): Evolution of the lithosphere mantle beneath the Marsabit volcanic field (northern Kenya): constraints from textural, P-T and geochemical studies on xenoliths. *J. Petrol.*, **47**, 2149-2184.

Kohler, T.P. & Brey, G.P. (1990): Calcium exchange between olivine and clinopyroxene calibrated as a geobarometer for natural peridotites from 2 to 60 kbar with applications. *Geochim. Cosmochim. Ac*ta, **54**, 2375-2388.

Mallick, D.I.S., Gass, I.G., Cox, K.G., De Vries, B.V.W., Tindle, A.G. (1990): Perim island, a volcanic remnant in the southern entrance to the Red Sea. *Geol. Mag.*, **127**, 309-318.

Meshesha, D. & Shinjo, R. (2007): Crustal contamination and diversity of magma sources in the northwestern Ethiopian volcanic province. *J. Miner. Petrol. Sci*., **102**, 272-290.

Meshesha, D. & Shinjo, R. (2010): Hafnium isotope variations in Bure volcanic rocks from the northwestern Ethiopian volcanic province: a new insight for mantle source diversity. *J. Miner. Petrol. Sci*., **105**, 101-111.

Natali, C., Beccaluva, L., Bianchini, G., Siena, F. (2011): Rhyolites associated to Ethiopian CFB: clues for initial rifting at the Afar plume axis. *Earth Planet. Sci. Lett.*, **312**, 59-68.

Natali, C., Beccaluva, L., Bianchini, G., Siena, F. (2013a): The Axum-Adwa basalt-trachyte complex: a late magmatic activity at the periphery of the Afar plume. *Contrib. Mineral. Petrol.*, **166**, 351-370.

Natali, C., Beccaluva, L., Bianchini, G., Ellam, R.M., Siena, F., Stuart, F.M. (2013b): Carbonated alkali-silicate metasomatism in the North Africa lithosphere: evidence from Middle Atlas spinel-lherzolites, Morocco. *J. South Am. Earth Sci.*, **41**, 113-121.

Niu, Y. (1997): Mantle melting and melt extraction processes beneath ocean ridges: evidence from abyssal peridotites. *J. Petrol*., **36**, 1047-1074.

Piccardo, G.B., Zanetti, A., Müntener, O. (2007): Melt/peridotite interaction in the Southern Lanzo peridotite: field, textural and geochemical evidence. *Lithos*, **94**, 181-209.

Pik, R., Daniel, C., Coulon, C., Yirgu, G., Hofmann, C., Ayalew, D. (1998): The northwestern Ethiopian flood basalts: classification and spatial distribution of magma types. *J. Volcanol. Geotherm. Res.*, **81**, 91-111.

Pik, R., Marty, B., Hilton, D.R. (2006): How many plumes in Africa? The geochemical point of view. *Chem. Geol*., **226**, 100-114.

Reisberg, L.C., Lorland, J.P., Bedini, R.M. (2004): Reliability of Os model ages in pervasively metasomatised continental mantle lithosphere: a case study of Sidamo spinel peridotites xenoliths (East African Rift, Ethiopia). *Chem. Geol.*, **208**, 119-140.

Rogers, N.W. (2006): Basaltic magmatism and geodynamics of the East African Rift System. *Geol. Soc. London, Spec. Publ.*, **259**, 77-93.

Shaw, J.E., Baker, J.A., Kent, A. J. R., Ibrahim, K.M., Menzies, M.A. (2007): The geochemistry of the Arabian Lithospheric mantle - a source for intraplate volcanism? *J. Petrol*., **48**, 1495-1512.

Stern, R.J. & Johnson, P. (2010): Continental lithosphere of the Arabian Plate: a geologic, petrologic, and geophysical synthesis. *Earth Sci. Rev*., **101**, 29-67.

Stracke, A., Hofmann, A., Hart, S. (2005): FOZO, HIMU, and the rest of the mantle zoo. *Geochem. Geophys. Geosyst.*, **6**, doi: 10.1029/2004GC000824.

Suhr, G. (1999): Melt migration under oceanic ridges: inferences from reactive transport modeling of upper mantle hosted dunites. *J. Petrol*., **40**, 575-599.

Sun, S.-S. & McDonough, W.F. (1989): Chemical and isotopic systematics of oceanic basalts: implications for mantle composition and process. *Geol. Soc. London, Spec. Publ.*, **42**, 313-346.

Teklay, M., Scherer, E.E., Mezger, K., Danyushevsky, L. (2010): Geochemical characteristics and Sr-Nd-Hf isotope compositions of mantle xenoliths and host basalts from Assab, Eritrea: implications for the composition and thermal structure of the lithosphere beneath the Afar depression. *Contrib. Mineral. Petrol.*, **159**, 731-751.

Toramaru, A. & Fujii, N. (1986): Connectivity of melt phase in a partially molten Peridotite*. J. Geophys. Res.*, **91**, 9239-9252.

White, W.M., Albarède, F., Télouk, P. (2000): High-precision analysis of Pb isotope ratios by multi-collector ICP-MS. *Chem. Geol.*, **167,** 257-270.

Zack, T. & Brumm, R. (1998): Ilmenite/liquid partition coefficients of 26 trace elements determined through ilmenite/clinopyroxene partitioning in garnet pyroxenites. 7$^{th}$ International Kimberlite Conference. Cape Town, 986-988.

Zindler, A. & Hart, S. (1986): Chemical geodynamics. *Ann. Rev. Earth Planet Sci.*, **14**, 493-571.